Fibers and Polymers
DOI 10.1007/s12221-022-0228-x

ISSN 1229-9197 (print version)
ISSN 1875-0052 (electronic version)

In Vitro Comparison Study of Plasma Treated Bilayer PGS/PCL and PGS/PLA Scaffolds for Vascular Tissue Engineering

Parisa Heydari[1,2], Shokoh Parham[1], Anousheh Zargar Kharazi[1,2]*, Shaghayegh Haghjooy Javanmard[2,3], and Seddigheh Asgary[3]*

[1]*Biomaterials Nanotechnology and Tissue Engineering Faculty, School of Advanced Technologies in Medicine, Isfahan University of Medical Sciences, Isfahan 81746, Iran*
[2]*Applied Physiology Research Center, Isfahan University of Medical Sciences, Isfahan 81746, Iran*
[3]*Isfahan Cardiovascular Research Center, Cardiovascular Research Institute, Isfahan University of Medical Sciences, Isfahan 81746, Iran*
(Received March 11, 2022; Revised May 6, 2022; Accepted May 10, 2022)

Abstract: Biomaterial selection is one of the important factors in tissue engineering vascular graft (TEVG) because of its hemocompatibility, mechanical properties, and biodegradability. In the present research, we prepared the bilayer electrospun scaffolds from poly glycerol sebacate (PGS)/poly caprolactone (PCL) and poly glycerol sebacate (PGS)/poly lactic acid (PLA), Then the surface of both groups was modified by using oxygen plasma. Physical, mechanical and hemocompatibility evaluation of the bilayer PGS/PCL and PGS/PLA scaffold was performed to introduce a more suitable combination for TEVG applications. Results demonstrated that the plasma treatment process did not affect the surface morphology of electrospinning fibers but improved hydrophilicity, swelling ratio, and blood compatibility. It caused a faster degradation rate in treated groups. Mechanical tests of these scaffolds showed a proper mechanical strength for vascular tissue engineering before and after plasma treatment, however, elongation of the PGS/PCL scaffolds was more suitable for vascular graft applications. The hemocompatibility study showed improvement in platelet adhesion, hemolysis, and blood clotting time after plasma treatment in both groups also, there was no significant difference between the two scaffolds in hemocompatibility characteristics. It concluded that the treated bilayer PGS/PCL scaffold can be more suitable for vascular graft application.

Keywords: Vascular grafts, Electrospinning, Plasma surface modification, PGS/PLA, PGS/PCL

Introduction

Cardiovascular defects are one of the most common reasons for mortality in the world [1]. In particular, coronary artery disorders are the main reason for death, accounting for 53 % of all deaths resulting from cardiovascular diseases [2]. Therefore, it is essential to look for ways to treat and inhibit disorders' development, in addition to their prevention. In many cardiac patients, veins in the body of the patients cannot be used for numerous reasons, such as the patient's age, small size, previous surgical procedure, or different disorders [3]. Therefore, it is necessary to find a blood vessel substitute; especially, vascular transplantation with a very small diameter, and proper substitutes can be helpful [4,5].

Nowadays, biomaterials play a significant role in biomedical sciences. Biodegradable and biocompatible biomaterials, such as Poly Caprolactone (PCL), Poly Glycerol Sebacate (PGS), Poly Lactic Acid (PLA), and their copolymers, have been widely used in medical research [6-8]. PGS is a colorless, degradable and flexible polyester, with mechanical properties appropriate for tissue substitution in the body [9]. PGS is used in tissue engineering of blood vessels, tissues and interstitial adhesives, extracellular matrices, and substitution of soft tissue organs [10,11]. PLA is a synthetic and hydrophobic polyester with a low degradation rate. The ideal mechanical and biological properties of this polymer, including biocompatibility, biodegradability, and non-toxic effects, have made it an appropriate candidate for biomedical and tissue engineering applications [11,12]. On the other hand, PCL is a hydrophobic semi-crystal polymer with excellent mechanical characteristics, high biocompatibility and poor antigenicity; it is used in medicine due to its flexible structure and long degradation time [13-15]. The suitable mechanical and elastic properties of the vessel are the important parameters for designing the proper scaffolds in vascular tissue engineering [5,16]. Therefore, PGS shows high flexibility, high hydrophilicity and good blood compatibility, and PLA or PCL can provide good mechanical strength. Therefore, the combination of PGS/PCL and PGS/PLA can lead to suitable applications in the field of vascular tissue engineering.

Electrospinning process is an interesting method to fabricate these grafts and achieve a TEVG ideal scaffold [17]. By applying the electrospinning technique, a multilayered nanofibrous scaffold with different properties at various layers can be fabricated to simulate the ability of the vessel natural tissue. In this regard, Vaz *et al*. produced a bilayered tubular scaffold of randomly oriented polycaprolactone (PCL) nanofibers as the inner layer and aligned poly(lactic

*Corresponding author: a_zargar@med.mui.ac.ir
*Corresponding author: sedighehasgary@gmail.com

acid) (PLA) nanofibers as the outer layer to provide enough strength and compliance required for vascular applications [18]. Ye *et al*. also fabricated a bilayered tubular scaffold consisting of PCL nanofibers in the inner layer and core-shell nanofibers encapsulating Bovine serum albumin (BSA) and tetrapeptide in the outer layer to release BSA and tetrapeptide that could enhance the cell growth [19].

Plasma treatment is a versatile and effective method for modifying the surface properties of a material without affecting its bulk properties [20]. One of the important effects of plasma treatment is surface cleaning, surface activation, and its effects on surface roughness. A common application of this technique is to improve surface hydrophilicity by forming oxygen-containing groups at the surface of the materials [12,21,22].

The aim of the present study was, therefore, to produce bilayer electrospun fibers of PGS/PCL and PGS/PLA in two groups before and after plasma surface treatment for vascular tissue engineering applications. The chemical structure, surface properties, physical properties, mechanical characteristics, and blood compatibility of the PGS/PCL and PGS/PLA scaffolds were studied and compared with each other.

Experimental

Materials

The materials used in this study were sebacic acid (99 %, Merck), glycerol (99 %, Merck), poly lactic acid (PLA) (Mw=200 kDa, Sigma-Aldrich), poly caprolactone (PCL) (Mw=8 kDa, Sigma-Aldrich), chloroform (Merck), acetone (Merck) and phosphate-buffered saline (PBS, Fisher Scientific, Gibco).

Polymer Synthesis, Electrospinning and Scaffolds Fabrication

Poly glycerol sebacate (PGS) was synthesized according to a previous protocol reported by Rai *et al.* [23]. To describe briefly, the PGS polymer was synthesized via condensation polymerization from Sebacic acid and glycerol.

A mixture of sebacic acid and glycerol at a molar ratio of 1:1 was heated at 120 °C for 24 hours under the N_2 atmosphere, and the reactant was kept under a vacuum at 40 °C for 24 hours. Finally, a white and viscous PGS polymer was obtained [23].

The electrospinning setting was adjusted on the JMS-model SP500 system (North America). The electrical power supply with a direct current was connected to the system.

First, to get the bilayer scaffold, the PCL with 18 % (w/v) concentration was prepared and stirred for 1 h in chloroform and acetone solvent with an 8:2 aspect ratio, respectively. PGS was then dissolved in these solvents at a 36 % (w/v) concentration for 30 min. after that the PCL and PGS solutions were mixed well for 15 min. After optimizing the electrospinning factor for the construction of bilayer scaffolds, PGS/PCL (2:1) solution as the inner layer and PCL were used in the outer layer. This scaffold was electrospun with the initial selection parameters (Needle size of 23 G, tip-to-collector distance of 18 cm), a voltage of 18 to 20 kV, feed flow rates of 1 m*l*/h, the temperature of 25±1 °C, and humidity of around 30 %. On the other hand, to prepare PGS/PLA with a total concentration of 9 % w/v, the PGS polymer was mixed with PLA at a weight ratio of 2:1 w/w in chloroform and acetone with an 8:2 aspect ratio as the inner layer; PLA was used in the outer layer at room temperature (26±1 °C), with the parameters of humidity (around 30 %) and Needle size (23 G), as well as initial selection parameters including tip-to-collector distance (15 cm), voltage (30 kV) and feed flow rates (0.8 m*l*/h).

Surface Modification of Electrospun Nanofibers

Oxygen plasma treatment of electrospun PGS/PCL and PGS/PLA fibers scaffolds was carried out by using radio-frequency (RF) plasma cleaner (SATIA knowledge-intensive company, USA). Nanofibers were placed in the chamber of the plasma cleaner and according to our previous research also similar studies plasma discharge was applied for 10 min, with the radio frequency power set as 20 under the vacuum mode [24,25].

Characterization of the Electrospun Scaffolds

Chemical Characterization

Fourier Transform Infrared spectroscopy (FTIR) (IFS-66 V/S, Bruker, Ettlingen, Germany) was used to analyze the chemical structure of PGS/PCL and PGS/PLA fiber scaffolds over the wavenumber range of 400 and 4000 cm^{-1}.

Morphology Analysis

Fiber morphology of PGS/PCL and PGS/PLA scaffolds with or without plasma treatment was evaluated by the scanning electron microscopy (SEM) device (EM3200-KYKY, Japan). Fiber diameters were measured using Image J (National Institutes of Health, USA). Average fiber diameter and size distribution were determined from approximately 30 random measurements by using micrographs representative of the fiber morphology. The porosity of the samples in SEM images was measured using the Matlab software (R 2016 a, The Mathworks Inc.) [26].

Water Contact Angle

The dynamic contact angle of the untreated and treated PGS/PCL and PGS/PLA samples was measured using an optical contact angle measuring device. The contact angle test was conducted by the drop model at a dosing volume of 4 μ*l*. The timer was started when the drop first touched the sample surface and it could be separated from the needle. Pictures were captured by the Charge Coupled Device (CCD) camera and the Image j software was used to determine the contact angles. The reported values were mean±standard deviation (n=3).

Water Uptake

The water uptake of the untreated and treated PGS/PCL and PGS/PLA fiber scaffolds was evaluated according to the ASTM D-5946 standard. First, the samples were cut (20 mm×5 mm); then the weight of each sample was measured (w_0) and each was immersed in deionized water separately [27]. After that, the wet weight (w_w) of the fibers was recorded (n=3). The percentage of water uptake was measured by using the following equation.

$$\text{Water uptake (\%)} = \frac{W_w - W_0}{W_0} \times 100 \quad (1)$$

where, W_0 is the fiber dry weight and W_w is the fiber wet weight.

In vitro Degradation

To study the degradation value of the fiber scaffolds, the samples were examined in the PBS solution. Toward this goal, the samples were cut (1 cm×1 cm dimensions and 200 μm thickness). Then the weight of each sample was recorded. After that, all samples were incubated for 8 weeks with 5 m*l* of PBS (37 °C, pH 7.4). The solution of each sample was changed every week. The scaffolds degradation test was performed in triplicate (n=3) [27]. After 8 weeks, the samples were removed from the PBS solution and washed with distilled water. The samples were then dried in a vacuum oven for 24 h. The weight loss percentage for each sample was measured by using the following equation:

$$\text{Weight loss (\%)} = \frac{W_0 - W_t}{W_0} \times 100 \quad (2)$$

where, W_t is the fiber dry weight after degradation at different times and W_0 is the fiber dry weight before degradation.

Mechanical Analysis

Mechanical properties including elastic modulus and tensile strength of the untreated and treated PGS/PCL and PGS/PLA fiber scaffolds were estimated according to the ASTM D882 standard. At first, electrospinning scaffolds were cut with the dimensions of 3 cm×1 cm; the thickness of every sample was about 300 μm. The tensile test was analyzed by using the Zwick/material testing machine (Zwick Co., Germany) (load cell=10 N and rate=5 mm/min). Every test was evaluated in triplicate (n=3).

Blood Compatibility

To study the blood compatibility of all samples, the hemolysis ratio, the degree of platelet adhesion and the whole blood clotting time were evaluated.

Hemolysis Ratio

Human whole blood was drawn from healthy adult volunteers (by the regulations of Isfahan University of Medical Sciences); Polytetrafluoroethylene (e-PTFE) and glass were used as negative and positive controls, respectively. The samples were cut (1 cm×1 cm) and placed in conical tubes (1.5 m*l*); then phosphate-buffered saline (PBS) and sterile distilled water were added separately to the conical tubes of positive and negative controls. After that, 200 μ*l* of fresh blood containing anticoagulant sodium citrate and 10 m*l* of normal saline (0.9 %) were added to each tube. The samples were incubated for 120 min (at 37 °C). The samples were then removed. After that, each tube was centrifuged for 10 min. All blood compatibility tests were carried out in three replicates (n=3). Then all sampled tubes were transferred to a 96-well plate and optical density was read by a spectrophotometric plate reader (BioTek, FLX800, wavelength= 540 nm). The hemolysis ratio was measured by using the following equation [24]:

$$\text{R (Hemolysis Ratio) (\%)} = \frac{A_{ts} - A_{nc}}{A_{pc} - A_{nc}} \times 100 \quad (3)$$

where, A_{nc}, A_{pc} and A_{ts} refer to the absorbance values of the negative control (Teflon), positive control (glass), and test sample, respectively.

Platelet Adhesion

The LDH (lactate dehydrogenase) activity assay kit (Biosystems reagents & Instruments) was used to determine the platelet adhesion degree of the fiber scaffolds according to the manufacturer's protocol. At first, 200 μ*l* of the human fresh PRP (platelet-rich plasma) was placed on the untreated and treated PGS/PCL and PGS/PLA scaffolds and e-PTFE and glass samples. The samples were then incubated for 120 min at 37 °C. The suspension of all incubated samples was removed; then they were washed with PBS three times and 40 μ*l* of Triton X-100 (1 %) solution was added to each sample for 30 min at 37 °C. After that, lysate (20 μ*l*) was added to the substrate solution (1 m*l*) containing pyruvate and NADH. Lactate dehydrogenase catalyzes the reduction of pyruvate by using NADH. Optical density was recorded at interval times (1-3 min). The concentration of LDH in the fiber samples was measured by using the following equation [24]:

$$\text{LDH concentration (U/L)} = \Delta A/\text{min} \times \frac{V_t \times 10^6}{\in \times L \times V_s} \quad (4)$$

where, the average of differences between consecutive absorbance is ΔA/min; the light path (L) equals 1 cm; the molar absorbance of NADH(ε) at 340 nm equals 6300; the sample volume (Vs) is 0.02 m*l* and the total reaction volume (Vt) is 1.02 m*l*.

Blood Clotting Time

To study the whole blood clotting time of the fiber scaffolds, e-PTFE and glass were selected as negative and positive controls; they were evaluated using a whole blood kinetic clotting time method [28]. First, 500 μ*l* of 0.03 M $CaCl_2$ (Sigma Aldrich) was added to the 5 m*l* of anticoagulant whole blood to activate the whole blood. Afterward, the samples were added to the 12-well plate with activated blood (100 m*l*). The samples were then incubated for 5, 10, 20, 30, 40, 50, and 60 min at atmospheric temperature. After

that, 2.5 m*l* of distilled water was added and 200 µ*l* of the suspension was removed from each sample; then it was transferred to a 96-well plate. The spectrophotometric plate reader (BioTek, FLX800, wavelength=540 nm) was used to measure the concentration of hemoglobin released in the solution. Optical density values were inversely related to the size of the clot plotted, according to the blood-contacting time. The anti-clotting index (ACI) of all samples was evaluated by using the following equation [29]:

$$ACI = \frac{OD\ of\ supernatant\ of\ blood\ with\ sample}{OD\ of\ citrated\ blood\ in\ distilled\ water} \times 100 \qquad (5)$$

Statistical Analysis

One-way ANOVA followed by a Least Square Difference test (LSD) was applied to analyze the results (statistically significant results: $p<0.05$). The results were obtained as mean±standard deviation.

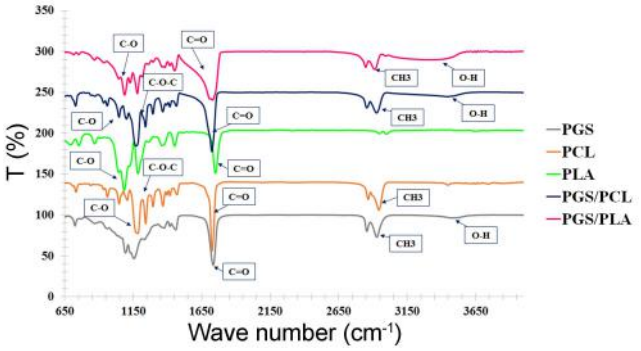

Figure 1. FTIR spectra of bilayer PGS/PCL and PGS/PLA scaffolds.

Results and Discussion

Chemical Characterization

Figure 1 shows the FTIR spectra PGS, PCL, PLA, bilayer PGS/PCL, and PGS/PLA scaffolds. The peaks included 1060 cm^{-1}, 1238 $cm^{-1,}$ and 1722 cm^{-1}, belonging to the C-O, C-O-C and C=O functional groups of the PCL polymer [30]. The peaks around 2925 cm^{-1} and 2853 cm^{-1} were related to methyl and alkane groups of the PGS polymers. The peak around 3458 cm^{-1} belonged to the hydroxyl group of two polymers and the ones at around 1171 cm^{-1} and 1731 cm^{-1} belonged to the C-O and C=O functional groups related to PGS [27,31]. Therefore, the FTIR spectrum of PGS/PCL revealed all of the specific bonds were related to PGS and PCL. The peaks around 2926, 1382 and 2854 cm^{-1} (methyl and alkane groups), 1738 cm^{-1} (ester carbonyl group), 1181 cm^{-1} (C-O stretching bond) and 3458 cm^{-1} belonged to the PGS polymers. Furthermore, the peaks around 753 cm^{-1} (C=O bending bond), 1088 cm^{-1} (C-O stretching bond), and 2292 cm^{-1} (hydroxyl group) belonged to the PLA polymer [24]. Also, the peaks around 3046 cm^{-1} (C-H stretching group) in the PLA polymer overlapped with the broad and wide peaks of PGS, and OH groups (3458 cm^{-1}). Therefore, these characteristic peaks demonstrated the combination of the PGS and PLA polymers in the PGS/PLA electrospun scaffold.

Fibers Morphology

The morphologies of the untreated and plasma-treated electrospun PGS/PCL and PGS/PLA fibers are shown in Figure 2. The diagram of the fiber diameter distribution was also provided by measuring the diameter of 30 fibers in the

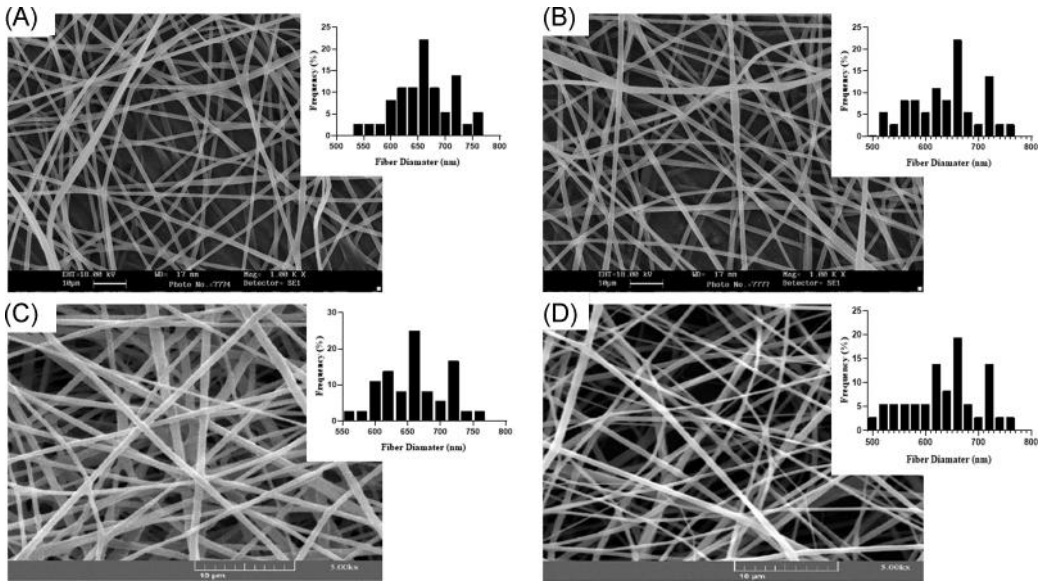

Figure 2. SEM micrographs of (A) PGS/PCL before plasma treatment, (B) PGS/PCL after plasma treatment, (C) PGS/PLA before plasma treatment, and (D) PGS/PLA after plasma treatment.

SEM images. The results are reported as mean±SD. According to Figure 2(A), the PGS/PCL fibers were bead free before plasma treatment, with a round shape; they were uniform with an average diameter of ~659±53 nm. The percentage of porosity was 91 %. On the other hand, oxygen plasma treatments analyzed by SEM revealed that the 10 min treatment with 20 W power created a suitable open space between the fibers still present in the mesh, and fibers with a regular morphology and a uniform diameter were observed. The fiber diameter in the treated PGS/PCL scaffold was about 625±96 nm and the microscopic characterization of this scaffold demonstrated a porous network structure (the percentage of porosity was 95 %) (Figure 2B). The SEM photomicrographs of the untreated and plasma-treated electrospun PGS/PLA fibers are shown in Figure 2(C, D). The results showed the average diameter of the electrospun PGS/PLA fibers before the treatment process in a relatively uniform size was about 638.9±62 nm; in the treated PGS/PLA sample, this was about 610±78 nm. The percentage of porosity in the untreated group was about 89 %; and in plasma-treated samples, this was 92 %. Based on the SEM images, plasma treatment did not change the surface morphology of the samples. There was no change in the open space between fibers, point-bonded junctions or melting of thinner fibers after plasma treatments. In other words, the results showed that after plasma treatment, the average diameter of the nanofibers was not considerably changed. Moreover, no considerable change was observed on the nanofiber surfaces in each group by using plasma surface modification ($p>0.05$). Mozafari *et al.* [32] also showed that the plasma treatment process did not affect the surface morphology of gelatin electrospinning fibers. Also, the fiber diameters result of PGS/PLA and PGS/PCL demonstrated that there was no significant difference between these groups ($p>0.05$), and these two groups had the same morphology and diameter of fibers.

The suitable percentage of surface porosity for the tissue engineering of vascular grafts was approximately 90 %, providing conditions similar to those of the natural vessels. The results of the present study were close to the above conditions [28]. In general, by obtaining the appropriate fiber diameter, it could be expected that the electrospun scaffold would be suitable in terms of biological behavior and blood compatibility [33].

Surface Hydrophilicity Analysis

Hydrophilicity essay is one of the main factors of biomaterial-cell interaction and biodegradation process in the first stage of contact. Figure 3 shows the hydrophilicity value of the untreated PGS/PCL and PGS/PLA samples in comparison with the treated PGS/PCL and PGS/PLA ones. The PGS had extremely high hydrophilicity' however, PCL and PLA had high hydrophobicity. As shown, the water contact angle of the untreated PGS/PCL composition was

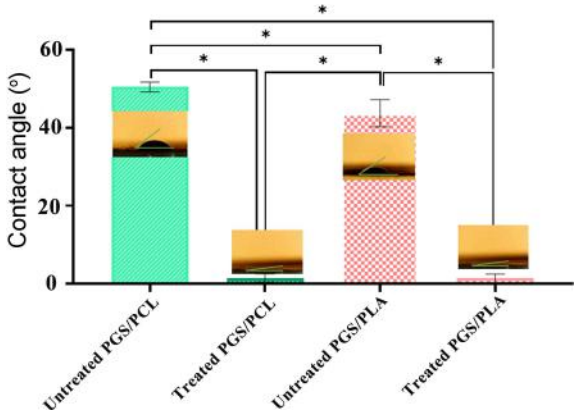

Figure 3. Water contact angle of nanofiber films before and after plasma treatment of PGS/PCL and PGS/PLA after contact for 10 seconds (n=3, * $p<0.05$).

about 51.5±5.8. After using plasma treating the surface of the PGS/PCL scaffold, the contact angle was d1ecreased to 0-7 °, and hydrophilicity was improved; so, it can be said that plasma treatment plays a critical role in improving the hydrophilicity of polymer surfaces. In the second part of the study, the untreated PGS/PLA scaffold showed a contact angle of about 45±2.8 degrees, thus confirming the hydrophilicity of this scaffold. The results of the contact angle test of PGS/PLA also showed that the surface treatment of this scaffold by plasma reduced the contact angle of the scaffold from 45 to 0 degrees. Therefore, e modification of the scaffold surface by plasma could improve the hydrophilicity of PGS/PLA and PGS/PCL fibers. Consequently, comparing the hydrophilicity test of the two scaffolds (PGS/PCL and PGS/PLA) showed that the hydrophilicity of PGS/PLA was more than that of PGS/PCL.

The hydrophilic parameter of the scaffold is important in the tissue culture, with an effect on the cell adhesion and initial migration [34,35]. PGS is a hydrophilic polymer due to the bonding of hydroxyl groups to other side chains in the polymer [36], whereas PCL and PLA are hydrophobic polymers [16,37]. Plasma surface modification of PGS/PCL and PGS/PLA scaffolds led to a reduction in the contact angle of the scaffolds from 51 (PGS/PCL) and 45 (PGS/PCL) to about 0 degrees. Oxygen plasma had a great influence on the surface of the two groups composite scaffold. By applying oxygen plasma to the surface, there was an increase in the interaction with carboxyl and carbonyl groups, which are largely polar and their presence provides a high level of surface polarity [24]. Therefore, plasma-surface modification by adding active functional groups (such as C-O and C=O) causes a change in surface morphology and surface charge, thus increasing the hydrophilicity of the scaffold [38,39].

According to a previous study, plasma surface modification of the fibers improved the scaffold surface properties and

significantly increased hydrophilicity; so, the growth and proliferation of HUVEC cells on the fibers could be improved [38,39]. As Mozaffari *et al.* demonstrated, plasma surface treatment was an ideal process to improve the hydrophilicity of nanofibers and acceleration the biomaterial's bio-functionality [40].

Water Uptake Analysis

The results of water uptake analysis showed the uptake rate of PGS/PCL scaffolds with and without the plasma treatment process was, on average, 120 % and 84 %, respectively (Table 1). In other groups, the uptake rate of the treated and untreated PGS/PLA scaffolds was, on average, 170 % and 89 %, respectively. The results were, thus, completely consistent with the contact angle test; this was because with increasing hydrophilicity due to surface modification, the reaction rate with water molecules was also raised, and water absorption was enhanced as well.

The main reason for the increase or decrease in the value of water uptake is hydrophilicity and the chemical interactions between the functional groups. So, the combination of PGS/PLA, which has more active types of hydroxyl, has higher hydrophilicity and more water absorption, as compared to PGS/PCL [41,42]. On the other hand, by modifying the surface by using oxygen plasma, the interactions between carbonyl and carboxylic groups in both groups were increased, leading to more hydrophilicity and better water absorption capacity [24,38]. In both groups, the surface plasma treatment of the samples leads to a suitable hydrophilic surface and swelling ratio. Previous studies reported that proper water absorption is important in vascular tissue engineering because it can prevent the loss of nutrients and is beneficial for cell growth and tissue regeneration [43,44].

Degradation Analysis

The degradation behavior of PGS/PCL and PGS/PLA scaffolds, before and after the plasma treatment process, was evaluated. The results of this analysis showed that the degradation of the scaffold after the treatment process in the PBS environment had a faster rate in comparison with the untreated sample in the PGS/PCL and PGS/PLA samples. According to Figure 4, the weight loss of the bilayer untreated PGS/PCL, treated PGS/PCL, untreated PGS/PLA, and treated PGS/PLA samples were about 14 %, 25 %, 19 %, and 29 % after 7 days. The Fast degradation in the initial days was due to the presence of PGS polymer in the structure, high water absorption, and surface degradation of this polymer [27,45]. After that, the degradation proceeds in a more stable so that, the weight loss of the bilayer untreated PGS/PCL sample was about 30 % after 60 days. The weight loss of the bilayer untreated PGS/PLA sample was about 34 %. After the plasma treatment process, the weight loss in PGS/PCL and PGS/PLA was about 45 and 46 percent, respectively. In the case of PGS/PLA and PGS/PCL, the results of the degradation test showed that the scaffolds had a faster degradation rate after plasma treatment during the 12 weeks. The results of the contact angle test of PGS/PLA and PGS/PCL also showed that surface treatment by plasma reduced the contact angle of the scaffolds. Therefore, modification of the scaffold's surface by plasma could improve the hydrophilicity of the fibers; by increasing the hydrophilicity of the fibers, the penetration of the PBS solution into the scaffolds was faster and the degradation rate was increased too.

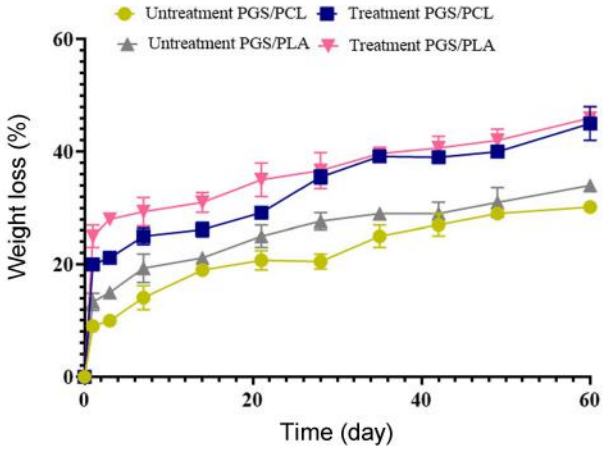

Figure 4. Degradation curves following soaking in PBS for PGS/PCL before and after plasma treatment, PGS/PLA before and after plasma treatment (n=3).

Table 1. Water uptake rate of samples after 24 hours of immersion in deionized water at 37 °C

Scaffolds	Water uptake rate (%)
PGS/PCL with plasma treated	120±12
PGS/PCL without plasma treated	84±14
PGS/PLA with plasma treated	170±22
PGS/PLA without plasma treated	89±9

So, the combination of PGS/PLA, which had more active types of hydroxyl groups, displayed higher hydrophilicity, more water absorption, and better interaction with water molecules, as compared to PGS/PCL [41,42]. This could be regarded as the cause of the faster degradation in the treated PGS/PLA scaffold, rather than the treated PGS/PCL. However, based on the comparison of these two membranes after surface modification in the process of degradation, it could be said that the degradation rate of treated PGS/PCL and PGS/PLA in this period time was not significantly different, with values close to each other.

It can be, therefore, concluded from this part that due to the modification of the scaffolding surface in both groups,

the amount of hydrophilicity, water absorption, and consequently, the rate of degradation was increased; however, the change in the degradation rate was increased by only 10 % and the specimen was not disintegrated after this period time (60 days).

Mechanical Properties

The tensile stress-strain curves of the untreated/treated PGS/PCL and PGS/PLA scaffolds have been shown in Figure 5. Other mechanical values such as tensile strength, elastic modulus, and elongation are reported in Table 2. The tensile strength of the untreated PGS/PCL and treated PGS/PCL scaffolds was equal to 0.81±0.09 and 0.77±0.1 MPa, respectively. On the other hand, the untreated and treated PGS/PLA scaffold had a tensile strength of about 1.3±0.12 and 0.89±0.14 MPa, respectively.

Therefore, the mechanical properties of the untreated and treated PGS/PCL and PGS/PLA were close to the proper mechanical properties of the natural vessels. These two scaffolds showed a mechanical strength suitable for preventing any fracture and rupture that could be deadly for the patient; therefore, these results could be regarded as one of the important advantages for vascular tissue engineering. Based on the previous studies, it can be said the elastic modulus for healthy arteries is at least 400 kPa. Elastic modulus and tensile strength values in this study could be suitable for vascular engineering [46].

It was shown that plasma treatment affected the mechanical properties of all samples. After plasma treatment, both ultimate tensile stress and young modulus of PGS/PLA and PGS/PCL were lower than those of the untreated samples. The elastic modulus of PGS/PCL was decreased from 4.8±0.1 MPa to 3.8±0.4 MPa after the treatment plasma process; the elastic modulus of PGS/PLA was decreased from 9.8±0.3 MPa to 5.9±0.9 MPa after treatment.

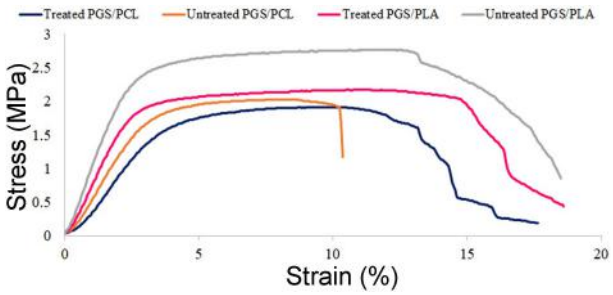

Figure 5. Stress-strain curve of untreated and plasma treated bilayer PGS/PCL and PGS/PLA electrospun scaffold (n=3).

Table 2. Tensile profiles of the treated and untreated PGS/PCL and PGS/PLA (n=3)

	Untreated PGS/PCL	Treated PGS/PCL	Untreated PGS/PLA	Treated PGS/PLA
Tensile strength (MPa)	0.81±0.09	0.77±0.1	1.3±0.12	0.89±0.14
Elastic modulus (MPa)	4.8±0.1	3.8±0.4	9.8±0.3	5.9±0.9
Elongation (%)	56±7.2	67±12.2	50±9.8	50±6.2

The decrease in ultimate tensile strength and elastic modulus after the plasma treatments could be attributed to the well-known plasma etching effects [38]. The effect of plasma etching is caused by the presence of oxygen ions and the reaction of these reactive ions with the chemical structure of the surface fibers, leading to some changes in the surface roughness of the nanofibers [47]. As shown by Mokhtari *et al.* [24], plasma surface modification could increase PGS/PLA fiber surface roughness and surface morphology changes.

Despite this slight reduction, both groups of scaffolds (untreated/treated PGS/PCL and PGS/PLA) still had ideal mechanical properties for vascular tissue engineering applications. However, based on the comparison of the two groups, the final tensile strength and Young's modulus in the PGS/PLA sample, in both cases, before and after the treatment process, were higher than those of the untreated and treated PGS/PCL membranes.

Blood Compatibility Study

The results of the LDH test were based on the activity of the lactate dehydrogenase enzyme, as shown in Figure 6(A) for the untreated and treated PGS/PCL, PGS/PLA scaffold, PTFE, and glass samples. According to the LDH results, there was a significant difference between the positive control group (glass) and the negative one (Teflon) with the untreated/treated PGS/PCL and untreated/treated PGS/PLA electrospun scaffold ($p<0.05$). The platelet cells were more sensitive to contact with the surface of the biomaterials, as compared with other blood cells. The LDH activity of the treated PGS/PCL electrospun scaffold was 0.37±0.08 at 540 nm. According to the obtained results, it can be said that the fiber morphology played a very important role in determining the rate of platelet adhesion to the scaffold surface. The LDH activity of the treated PGS/PLA scaffold was 0.48±0.06. A comparison of the treated PGS/PCL scaffolds and the treated PGS/PLA sample showed that the level of LDH activity was very close; as shown in the figure, there was no significant difference between these two treated groups ($p>0.05$). According to the obtained results, the surface modification by plasma decreased the platelet adhesion in each of the groups. These could be attributed to the effect of active functional groups and the increase of hydrophilicity. Platelet adhesion is the beginning of thrombosis and a gradual decrease in blood flow, ultimately leading to vascular occlusion [48].

The results of the hemolysis of PGS/PCL and PGS/PLA before and after the plasma treatment process are demonstrated in Figure 6(B). The percentage of damage and lysis of the

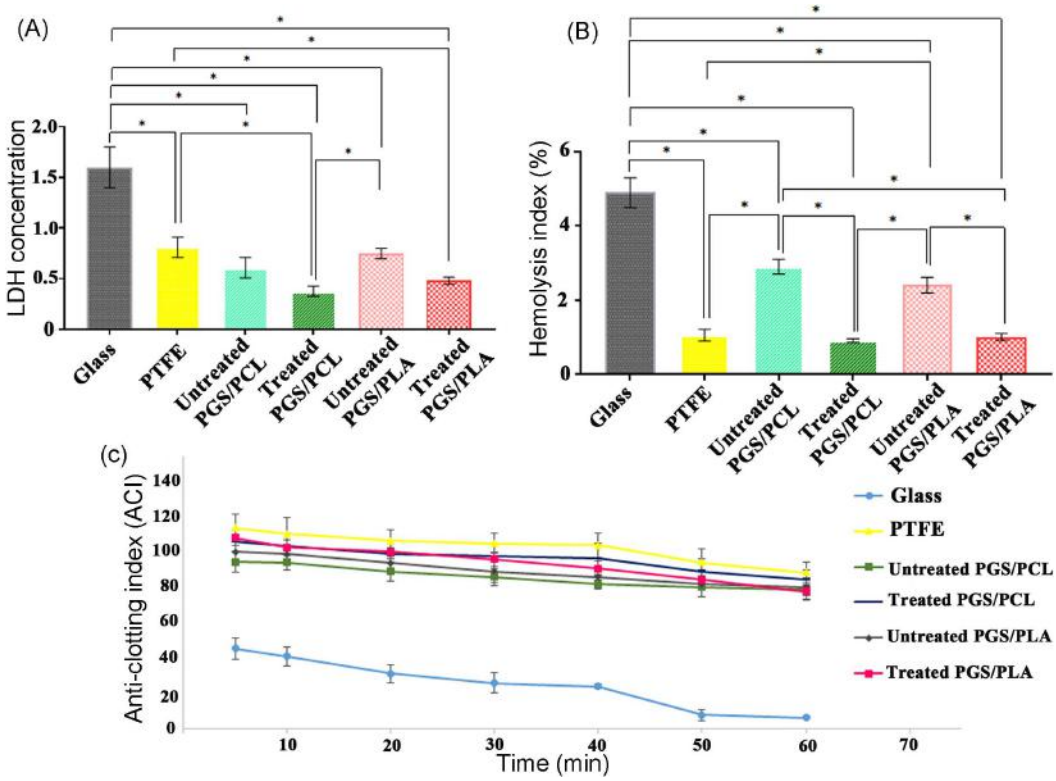

Figure 6. Blood compatibility evaluation of untreated and treated PGS/PCL and PGS/PLA scaffolds, e-PTFE, and glass samples; (A) platelet adhesion, (B) hemolysis ratio, and (C) blood clotting profiles, (*): $p<0.05$.

red blood cells in the presence of untreated PGS/PCL, untreated PGS/PLA, treated PGS/PCL, treated PGS/PLA scaffolds, positive and negative control samples was 2.9±1.2, 2.4±0.2, 0.9±0.05,1±0.09, 4.91±0.41 and 1.02±0.13, respectively. According to the previous studies, a hemolysis rate of less than 2 % is very desirable for vascular applications [49]. Therefore, the treated PGS/PCL and PGS/PLA scaffold showed very favorable conditions in terms of hemolysis due to its hydrophilicity, and uniform and smooth fibers. Based on the results, the scaffold with plasma treatment showed very good conditions in terms of the hemolysis rate. Overall, it can be said that the tested scaffolds with plasma treatment showed no hemolysis; therefore, they are suitable for use in vascular tissue engineering. Also, the results of this study showed that hemolysis was the same in the treated PGS/PCL and PGS/PLA scaffolds, and there was no significant difference between the two groups.

In the last part of the blood compatibility tests, the results of the blood clotting of the PGS/PCL, PGS/PLA scaffolds, before and after plasma treatment, glass, and Teflon as positive and negative control are shown in Figure 6(C). Clearly, there was no significant difference between the groups of electrospun scaffolds before plasma treatment, as compared to the scaffolds after plasma treatment and negative control (Teflon) in blood clotting. In other words, the level of blood clotting in the untreated and treated PGS/PLA and PGS/PCL samples was suitable, such as Teflon in vascular tissue engineering.

Blood clotting in the presence of biologic scaffolds is considered the peak undesirable effect of the scaffold's blood compatibility, which is the beginning of a coagulation cascade [50]. In bilayer scaffolds, before and after surface treatment, hydroxyl and carbonyl groups on the polymer surface increased the polarity of the surface, and enhancing oxygen at the surface reduced coagulation activation [51,52].

In general, the results of blood compatibility tests in the present study demonstrated that both PGS/PCL and PGS/PLA samples, especially after the plasma surface treatment process, showed the compatibility of blood cell behaviors by increasing hydrophilicity and adding new chemical groups on the surface. On the other hand, the results of blood compatibility in LDH activity, hemolysis, and blood clotting showed that the treated PGS/PCL and PGS/PLA, were close to each other; in fact, there was no significant difference between these two groups.

Conclusion

In this study, two bilayer scaffolds were made from PGS/PCL and PGS/PLA via the electrospinning method and then

treated by plasma technology. The chemical, physical and biological properties of the untreated and treated bilayer PGS/PCL and PGS/PLA scaffolds were evaluated. Morphological properties of these samples showed the smooth and free-bead fibers before and after the treatment process. The results also demonstrated the plasma treatment process improved the physical properties. The hydrophilicity of the treated scaffolds was more than that of the untreated ones in the two groups. Therefore, the swelling and degradation rate of the treated PGS/PLA and PGS/PCL scaffolds was faster than that of the untreated ones. Studies on the mechanical properties of these two samples also showed that in both cases, before and after plasma surface modification, the mechanical properties of bilayer membranes could be suitable for vascular applications. Comparison of PGS/PCL and PGS/PLA also showed that the treated PGS/PLA had a higher ultimate tensile strength and elastic modulus when compared to the untreated and treated PGS/PCL. The blood compatibility study also showed the low rate of platelet adhesion to the scaffold surface, the lowest hemolysis rate of red blood cells in contact with the scaffolds, and the best blood clotting time in the presence of both electrospun scaffolds. Therefore, based on these results, the blood compatibility of the treated PGS/PLA and PGS/PCL scaffolds was similar and suitable for use in vascular tissue engineering.

Acknowledgments

This research study has been supported by funding from the NIMAD (National Institute for Medical Research Development Islamic Republic of Iran) grant.

Conflict of Interest

The authors declare no conflict of interest.

References

1. H. G. Song, R. T. Rumma, C. K. Ozaki, E. R. Edelman, and C. S. Chen, *Stem Cell*, **22**, 340 (2018).
2. S. Aslani, M. Kabiri, M. Kehtari, and H. Hanaee-Ahvaz, *J. Cell. Physiol.,* **234**, 16080 (2019).
3. L. Soletti, Y. Hong, J. Guan, J. J. Stankus, M. S. El-Kurdi, W. R. Wagner, and D. A. Vorp, *Acta Biomater*., **6**, 110 (2010).
4. D. G. Seifu, A. Purnama, K. Mequanint, and D. Mantovani, *Nat. Rev. Cardiol.,* **10**, 410 (2013).
5. V. Catto, S. Farè, G. Freddi, and M. C. Tanzi, *International Scholarly Research Notices,* **2014**, 923030 (2014).
6. H. M. Aydin, K. Salimi, M. Yilmaz, M. Turk, Z. M. O. Rzayev, and E. Pişkin, *J. Tissue Eng. Regen. Med*., **10**, E14 (2016).
7. S. H. Javanmard and J. Anari, *J. Biomater. Appl.,* **31**, 438 (2016).
8. A. Ehterami, M. Salehi, S. Farzamfar, A. Vaez, H. Samadian, H. Sahrapeyma, M. Mirzaii, S. Ghorbani, and A. Goodarzi, *Int. J. Biol. Macromol*., **117**, 601 (2018).
9. S. Sant, D. Iyer, A. K. Gaharwar, A. Patel, and A. Khademhosseini, *Acta Biomater*., **9**, 5963 (2013).
10. S. Sant, C. M. Hwang, S.-H. Lee, and A. Khademhosseini, *J. Tissue Eng. Regen. Med*., **5**, 283 (2011).
11. B. Xu, B. Rollo, L. A. Stamp, D. Zhang, X. Fang, D. F. Newgreen, and Q. Chen, *Biomaterials*, **34**, 6306 (2013).
12. I. Armentano, G. Ciapetti, M. Pennacchi, M. Dottori, V. Devescovi, D. Granchi, N. Baldini, B. Olalde, M. J. Jurado, and J. I. M. Alava, *J. Appl. Polym. Sci*., **114**, 3602 (2009).
13. A. K. Gaharwar, S. Mukundan, E. Karaca, A. Dolatshahi-Pirouz, A. Patel, K. Rangarajan, and A. Khademhosseini, *Tissue Eng. Part A*, **20**, 2088 (2014).
14. A. K. Gaharwar, M. Nikkhah, S. Sant, and A. Khademhosseini, *Biofabrication*, **7**, 15001 (2014).
15. A. Gholipour Kanani and S. Hajir Bahrami, *J. Nanomater*., **2011**, 724153 (2011).
16. J. Dou, Y. Wang, X. Jin, P. Li, L. Wang, J. Yuan, and J. Shen, *Mater. Sci. Eng. C*, **107**, 110246 (2020).
17. C. Huang, X. H. Geng, K. Qin-Fei, M. Xiu-Mei, S. S. Al-Deyab, and M. El-Newehy, *Prog. Nat. Sci. Int.*, **22**, 108 (2012).
18. C. M. Vaz, S. Van Tuijl, C. V. C. Bouten, and F. P. T. Baaijens, *Acta Biomater*., **1**, 575 (2005).
19. L. Ye, J. Cao, L. Chen, X. Geng, A. Zhang, L. Guo, Y. Gu, and Z. Feng, *J. Biomed. Mater. Res. Part A*, **103**, 3863 (2015).
20. M. Parvinzadeh Gashti, D. Hegemann, M. Stir, and J. Hulliger, *Plasma Process. Polym*., **11**, 37 (2014).
21. A. D. Hanson, M. E. Wall, B. Pourdeyhimi, and E. G. Loboa, *J. Biomater. Sci. Polym. Ed.*, **18**, 1387 (2007).
22. A. Martins, E. D. Pinho, S. Faria, I. Pashkuleva, A. P. Marques, R. L. Reis, and N. M. Neves, *Small*, **5**, 1195 (2009).
23. R. Rai, M. Tallawi, A. Grigore, and A. R. Boccaccini, *Prog. Polym. Sci.*, **37**, 1051 (2012).
24. N. Mokhtari and A. Zargar Kharazi, *J. Biomed. Mater. Res. Part A*, **109**, 2673 (2021).
25. D. M. Correia, C. Ribeiro, V. Sencadas, G. Botelho, S. A. C. Carabineiro, J. L. G. Ribelles, and S. Lanceros-Méndez, *Prog. Org. Coatings*, **85**, 151 (2015).
26. L. Ghasemi-Mobarakeh, D. Semnani, and M. Morshed, *J. Appl. Polym. Sci.*, **106**, 2536 (2007).
27. P. Heydari, J. Varshosaz, A. Zargar Kharazi, and S. Karbasi, *Polym. Adv. Technol*., **29**, 1795 (2018).
28. J. P. Cuenca, A. Padalhin, and B.-T. Lee, *Mater. Lett*., **284**, 128973 (2021).
29. N. Tran, A. Le, M. Ho, N. Dang, H. H. Thi Thanh, L. Truong, D. P. Huynh, and N. T. Hiep, *Sci. Technol. Adv. Mater.*, **21**, 56 (2020).

30. K. K. Gómez-Lizárraga, C. Flores-Morales, M. L. Del Prado-Audelo, M. A. Álvarez-Pérez, M. C. Piña-Barba, and C. Escobedo, *Mater. Sci. Eng. C*, **79**, 326 (2017).
31. M. Kharaziha, M. Nikkhah, S.-R. Shin, N. Annabi, N. Masoumi, A. K. Gaharwar, G. Camci-Unal, and A. Khademhosseini, *Biomaterials*, **34**, 6355 (2013).
32. A. Mozaffari, M. Parvinzadeh Gashti, M. Mirjalili, and M. Parsania, *Membranes*, **11**, 31 (2021).
33. A. Z. Kharazi, M. Atari, E. Vatankhah, and S. H. Javanmard, *Polym. Adv. Technol.*, **29**, 3151 (2018).
34. S. Salehi, M. Fathi, S. H. Javanmard, T. Bahners, J. S. Gutmann, S. Ergün, K. P. Steuhl, and T. A. Fuchsluger, *Macromol. Mater. Eng.*, **299**, 455 (2014).
35. P. Heydari, A. Zargar Kharazi, S. Asgary, and S. Parham, *J. Biomed. Mater. Res. Part A*, **110**, 341 (2022).
36. A. Fakhrali, M. Nasari, N. Poursharifi, D. Semnani, H. Salehi, M. Ghane, and S. Mohammadi, *J. Appl. Polym. Sci*., **138**, 51177 (2021).
37. A. A. Aldana, L. Malatto, M. Atiq, U. Rehman, A. R. Boccaccini, and G. A. Abraham, *Nanomaterials*, **9**, 120 (2019).
38. D. Yan, J. Jones, X. Y. Yuan, X. H. Xu, J. Sheng, J. Lee, G. Q. Ma, and Q. S. Yu, *J. Biomed. Mater. Res. Part A*, **101**, 963 (2013).
39. E. D. Yildirim, D. Pappas, S. Güçeri, and W. Sun, *Plasma Process. Polym*., **8**, 256 (2011).
40. A. Mozaffari and M. Parvinzadeh Gashti, *Biomedicines*, **10**, 617 (2022).
41. R. M. Aghdam, S. Najarian, S. Shakhesi, S. Khanlari, K. Shaabani, and S. Sharifi, *J. Appl. Polym. Sci.,* **124**, 123 (2012).
42. H. Qi, Z. Ye, H. Ren, N. Chen, Q. Zeng, X. Wu, and T. Lu, *Life Sci*., **148**, 139 (2016).
43. L. Yang, X. Li, D. Wang, S. Mu, W. Lv, Y. Hao, X. Lu, G. Zhang, W. Nan, and H. Chen, *J. Biomater. Sci. Polym. Ed*., **31**, 658 (2020).
44. F. Ghorbani, H. Nojehdehyan, A. Zamanian, M. Gholipourmalekabadi, and M. Mozafari, *Adv. Mater. Lett*., **7**, 163 (2016).
45. S.-L. Liang, X.-Y. Yang, X.-Y. Fang, W. D. Cook, G. A. Thouas, and Q.-Z. Chen, *Biomaterials*, **32**, 8486 (2011).
46. S. Gorgani, A. Zargar Kharazi, S. Haghjooy Javanmard, and M. Rafiinia, *J. Polym. Environ.,* **28**, 2352 (2020).
47. P. Verdonck, P. B. Calíope, E. D. M. Hernandez, and A. N. R. da Silva, *Thin Solid Films*, **515**, 831 (2006).
48. D. Motlagh, J. Allen, R. Hoshi, J. Yang, K. Lui, and G. Ameer, *J. Biomed. Mater. Res. Part A*, **82**, 907 (2007).
49. S. N. Banitaba, A. A. Gharehaghaji, and A. A. A. Jeddi, *Bull. Mater. Sci.,* **44**, 1 (2021).
50. Z.-J. Sun, L. Wu, W. Huang, X.-L. Zhang, X.-L. Lu, Y.-F. Zheng, B.-F. Yang, and D.-L. Dong, *Mater. Sci. Eng. C,* **29**, 178 (2009).
51. Y.-C. Tyan, J.-D. Liao, R. Klauser, I.-D. Wu, and C.-C. Weng, *Biomaterials,* **23**, 65 (2002).
52. M. P. Prabhakaran, J. Venugopal, C. K. Chan, and S. Ramakrishna, *Nanotechnology*, **19**, 455102 (2008).